JPET Fast Forward. Published on January 8, 2013 as DOI: 10.1124/jpet.112.201616

Title Page

A G protein-biased ligand at the μ-opioid receptor is potently analgesic with reduced gastrointestinal and respiratory dysfunction compared to morphine

Scott M. DeWire, Dennis S. Yamashita, David H. Rominger, Guodong Liu, Conrad L. Cowan, Thomas M. Graczyk, Xiao-Tao Chen, Philip M. Pitis, Dimitar Gotchev, Catherine Yuan, Michael Koblish, Michael W. Lark, and Jonathan D. Violin

Trevena Inc, 1018 West 8th Avenue, Suite A, King of Prussia PA 19406

JPET Fast Forward. Published on January 8, 2013 as DOI: 10.1124/jpet.112.201616
This article has not been copyedited and formatted. The final version may differ from this version.

Running Title Page (60 characters max)

TRV130: a μ-opioid receptor biased ligand

Corresponding author: Jonathan Violin, Trevena Inc, 1018 West 8th Ave, Suite A, King of Prussia PA 19406. Phone: 610-354-8840; Fax: 610-354-8850; email: jviolin@trevenainc.com

Text pages: x
Tables: 2 plus 5 supplemental
Figures: 8 plus 6 supplemental
References: 56 (60 max)
Abstract: 163 (250 max)
Introduction: 729 (750 max)
Discussion: 1066 (1500 max)

Non-standard Abbreviations and Acronyms

GPCR, G protein-coupled receptor
MOR: μ-opioid receptor
KOR: κ-opioid receptor
DOR: δ-opioid receptor
NOP: nociceptin receptor (aka ORL-1)
KO: knock out
DAMGO: [D-Ala2, NMe-Phe4, Gly-ol^5]-enkephalin
cAMP: cyclic adenosine monophosphate
GRK: G protein coupled receptor kinase

Recommended section assignment: Neuropharmacology

JPET Fast Forward. Published on January 8, 2013 as DOI: 10.1124/jpet.112.201616
This article has not been copyedited and formatted. The final version may differ from this version.

Abstract

The concept of ligand bias at G protein-coupled receptors broadens the possibilities for agonist activities and provides the opportunity to develop safer, more selective therapeutics. Morphine pharmacology in β-arrestin2 knock out mice suggested that a ligand that promotes coupling of the μ-opioid receptor (MOR) to G proteins, but not β-arrestins, would result in higher analgesic efficacy, less gastrointestinal dysfunction, and less respiratory suppression than morphine. Here we report the discovery of TRV130 ([(3-methoxythiophen-2-yl)methyl]({2-[(9R)-9-(pyridin-2-yl)-6-oxaspiro[4.5]decan-9-yl]ethyl})amine), a novel MOR G protein-biased ligand. In cell-based assays, TRV130 elicits robust G protein signaling, with potency and efficacy similar to morphine, but with far less β-arrestin recruitment and receptor internalization. In mice and rats, TRV130 is potently analgesic while causing less gastrointestinal dysfunction and respiratory suppression than morphine at equianalgesic doses. TRV130 successfully translates evidence that analgesic and adverse MOR signaling pathways are distinct into a biased ligand with differentiated pharmacology. These preclinical data suggest that TRV130 may be a safer and more tolerable therapeutic for treating severe pain.

Introduction

Morphine is the archetypal opioid (Hamilton and Baskett, 2000) and is still considered a mainstay of analgesic therapy. It elicits analgesia by stimulating the μ-opioid receptor (MOR), a G protein coupled receptor (GPCR) highly expressed in the central nervous system and gastrointenstinal tract. While extremely efficacious at relieving pain, opioids, as a class, also elicit a wide array of adverse events including respiratory suppression, sedation, and gastrointestinal dysfunction including nausea, vomiting, and constipation. In addition, the euphoria and physical dependence associated with opioids can lead to abuse and addiction. Furthermore, patients can develop tolerance to opioid analgesia, necessitating dose escalation and risking worsening tolerability (Schneider and Kirsh, 2010). In the post-operative setting,

JPET Fast Forward. Published on January 8, 2013 as DOI: 10.1124/jpet.112.201616
This article has not been copyedited and formatted. The final version may differ from this version.

where opioids are widely used, nausea and vomiting delay recuperation and hospital discharge, as can opioid-induced constipation, especially in cases of post-operative ileus (Marderstein and Delaney, 2008). In addition, although opioid-induced respiratory suppression is rare, risk of its occurrence limits dosing (Dahan, 2007), contributing to the 29% of patients who report post-operative pain despite opioid use (Bostrom et al., 1997). In the outpatient settings of acute and chronic pain, the same array of undesirable pharmacologies exists. Constipation lowers the quality of life for over half of patients taking oxycodone for chronic pain (Anastassopoulos et al., 2011) and can be dose-limiting as many patients would rather suffer reduced analgesia than continue opioid use and contend with serious gastrointestinal discomfort. Furthermore, respiratory suppression can be fatal in cases of overdose, and is associated with nearly 15,000 deaths per year, a number that has escalated as opioid prescriptions have increased in recent years (Manchikanti et al., 2012).

These adverse pharmacologic responses are elicited by all marketed opioid analgesics, and have long been considered an immutable feature of strong MOR agonists. In rodents, these effects are reversible by MOR antagonists and absent in MOR knockout animals (Matthes et al., 1996; Sora et al., 1997; Kieffer, 1999), indicating they are “on-target” and cannot be improved by increasing receptor selectivity. However, numerous studies have shown that not all downstream signaling activities of a GPCR act with parallel, equivalent efficacies (Kenakin, 2011). Indeed, signal selectivity at a receptor can be targeted pharmacologically; “biased ligands” stabilize conformations that preferentially couple the receptor to particular intracellular pathways without coupling to others (Kenakin, 2011; Rajagopal et al., 2011). In extreme cases, a biased ligand is equivalent to a full agonist reference compound for one pathway, but is inert, or even displays inverse efficacy in another pathway stimulated by the reference ligand. Such a ligand, in a physiological setting of an endogenous circulating agonist, can stimulate some receptor responses while inhibiting others (Violin et al., 2010; Kenakin, 2011). GPCR ligand bias has been observed between a number of intracellular signaling pathways, including coupling to different Gα subunits (Spengler et al., 1993; Eason et al., 1994), and between G protein coupling and β-arrestin

JPET Fast Forward. Published on January 8, 2013 as DOI: 10.1124/jpet.112.201616
This article has not been copyedited and formatted. The final version may differ from this version.

recruitment (Azzi et al., 2003; Gesty-Palmer et al., 2006; DeWire et al., 2007; Violin and Lefkowitz, 2007; Kim et al., 2008; Ma et al., 2009; Gesty-Palmer and Luttrell, 2011; Rosethorne and Charlton, 2011).

Evidence from knockout (KO) mice suggests that opioids signal through distinct MOR pathways, indicating that ligand bias might elicit differential MOR pharmacology. In β-arrestin2 KO mice, morphine analgesia was enhanced and prolonged compared to morphine in wild type littermates (Bohn et al., 1999). Similar findings were noted in both mice and rats following injection of β-arrestin2 interfering RNAs to specific brain regions (Li et al., 2009; Yang et al., 2011). In contrast, morphine-induced constipation, respiratory suppression, and tolerance were each reduced in β-arrestin2 KO mice versus wild type animals (Raehal et al., 2005). Thus at the MOR, β-arrestins serve as negative modulators of analgesia and positive modulators of some MOR-mediated adverse effects such as constipation, tolerance, and respiratory suppression. This is consistent with the understanding that β-arrestins not only desensitize a receptor's G protein-mediated signaling, but also stimulate distinct and independent cell signaling outcomes (Wei et al., 2003; Rajagopal et al., 2006; Gesty-Palmer et al., 2009; Violin et al., 2010; Allen et al., 2011; DeWire and Violin, 2011; Audet et al., 2012).

It remains unclear if a G protein-biased ligand at the MOR can successfully recapitulate the improved profile of morphine in β-arrestin2 KO mice. We sought to discover and characterize such a biased MOR ligand to test this possibility in hopes of developing a safer, better tolerated, and more efficacious opioid analgesic.

Methods

Drugs and chemicals:

TRV130 hydrochloride and trifluoroacetate were synthesized by the chemistry group of Trevena Inc as described elsewhere (Yamashita et al, *manuscript in preparation*). [D-Ala2, NMe-Phe4, Gly-ol^{5}]-

JPET Fast Forward. Published on January 8, 2013 as DOI: 10.1124/jpet.112.201616
This article has not been copyedited and formatted. The final version may differ from this version.

enkephalin (DAMGO) and buprenorphine were purchased from Tocris (Bristol, UK). Fentanyl, morphine, and oxycodone were purchased from Sigma-Aldrich (St, Louis, MO).

In vivo studies:

Analgesia studies were performed at Trevena Inc. with either male C57BL/6J mice or male Sprague-Dawley rats (Hilltop Lab Animals, Inc., Scottsdale, PA) housed in standard conditions with a 12-hr light/dark cycle. Assays were approved by the Institutional Animal Care and Use Committee and were carried out in accordance with the *Guide for the Care and Use of Laboratory Animals* as adopted by the U.S. National Institutes of Health. Studies of respiratory suppression were performed at Calvert Labs (Scott Township, PA), and pharmacokinetics studies were performed at ChemPartner Co (Shanghai, China), under protocols reviewed and approved by the respective Institutional Animal Care and Use Committees.

***Cell culture and preparation*:**

HEK-293 cells stably transfected to overexpress β-arrestin2 fused to a β-galactosidase fragment were purchased from DiscoveRx (PathHunter β-arrestin assay, DiscoveRx Corporation, Fremont California) and the human OPRM1 gene (NM_000914.3, encoding human MOR), mouse OPRM1 gene (NM_001039652.1, mouse MOR), rat OPRM1 gene (NM_001038597.2, rat MOR), dog OPRM1 gene (XM_003638781, dog MOR), human OPRD1 gene (NM_000911.3, human DOR), human OPRK1 gene (NM_000912.3, human KOR) and human OPRL1 gene (NM_182647.2, human NOP/ORL-1) receptors were fused to a complementary β-galactosidase fragment using the pCMV-ProLink plasmid purchased from DiscoveRx. Cells were grown in MEM with 10% FBS, 1% penicillin/streptomycin, and 150 µg/L of neomycin and 150 µg/L of hygromycin.

β-arrestin2 recruitment:

The PathHunter enzyme complementation assay (DiscoveRx Corporation, Fremont, California) was performed according to the manufacturer's protocol, and read for chemiluminescence on a PheraStar plate reader (BMG Labtech, Durham, North Carolina). Briefly, when β-arrestin2 translocates to active

JPET Fast Forward. Published on January 8, 2013 as DOI: 10.1124/jpet.112.201616
This article has not been copyedited and formatted. The final version may differ from this version.

receptor, the complementary β-galactosidase fragments fused to receptor and β-arrestin interact to form a functional enzyme, which is detected by chemiluminescence. For all in vitro assays, data were normalized as a percentage of maximal assay responses, typically defined by DAMGO stimulated activity in the MOR assays, unless indicated otherwise.

cAMP accumulation:

Receptor G-protein mediated responses were determined by measuring changes in cAMP using the cAMP-HTRF kit (Cisbio, Codolet, France), using the same cell lines as used to measure β-arrestin recruitment. MOR, KOR, DOR, and NOP all couple to Gαi so G protein coupling was measured as inhibition of forskolin-stimulated cAMP accumulation in the presence of 1.5 mM NKH-477 (water-soluble forskolin, Tocris catalog #1603) and 500uM 3-Isobutyl-1-methylxanthine (IBMX). cAMP accumulation assays were run in parallel with β-arrestin2 recruitment, using the same cells, drug dilutions, and assay buffers (1% DMSO, F12 Ham's buffer) to ensure accurate assay-to-assay comparisons of data. Plates were read using a time-resolved fluorescence ratio (665nm/620nm) on a PheraStar plate reader.

Internalization assay:

The PathHunter GPCR Internalization assay (DiscoveRx Corporation, Fremont, CA) was performed according to the manufacturer's protocol. Briefly, U2-osteosarcoma (U2-OS cells) stably expressing the human MOR with complementary pieces of β-galactosidase were genetically fused to the receptor and a component of the endocytic vesicle, respectively. When co-expressed, the two fusion proteins detect receptor localization to endosomes, detected by chemiluminescence.

Immunoblotting:

HEK-293 cells stably expressing the human MOR were grown in MEM supplemented with 10% FBS. After overnight serum starvation, cells were stimulated with 1 μM DAMGO, morphine, fentanyl, TRV130, or vehicle for 5 minutes. Lysates were fractionated by SDS PAGE, transferred to nitrocellulose membranes, and immunoblotted with phospho-MOR serine 375 antibody per manufacturer's instructions (Cell Signaling Technologies, Danvers, Massachusetts, catalog number

JPET Fast Forward. Published on January 8, 2013 as DOI: 10.1124/jpet.112.201616
This article has not been copyedited and formatted. The final version may differ from this version.

3451). The immunoreactive band for the MOR was visualized and quantified using GeneSnap and GeneTools software (Syngene USA, Frederick, Maryland).

Radioligand binding assays:

Equilibrium binding of unlabeled compounds was measured by inhibition of radioligand binding ([^{3}H]-diperenorphine) to HEK cell membranes expressing human MOR, KOR and DOR. Unlabeled ligand and buffer (50 mM Hepes, 5mM MgCl2, 1 mM EGTA and 0.05% Bovine serum albumin pH 7.2 at 23^{o}C) containing radioligand were added to polypropylene 96 well plates (Costar Corp., Cambridge, MA). Assays were initiated by the addition of membrane (5-10 µg protein/well) suspension. The concentration of [^{3}H]-diprenorphine, specific activity 50-52 Ci/mmol; PerkinElmer Life and Analytical Sciences, Boston, MA), was 0.5-1 times K_d. Compounds were diluted in DMSO and tested at a final concentration of 1% DMSO. Nonspecific binding was defined in the presence of 1µM naloxone. Competition assays were performed at 23°C for 3-4 hours to allow adequate time for equilibrium binding. In all assays, total radioligand bound to the filter was less than 10% of the total radioligand added. The separation of bound from free radioligand was accomplished by rapid vacuum filtration of the incubation mixture over GF/B filter mats using a Brandel cell harvester (Brandel, Gaithersburg, MD). Filters were washed 2 times with 0.5 ml of ice-cold phosphate buffered saline pH 7.0 containing 0.01% Triton X100. Radioactivity on the filters was quantified using a MicroBeta TriLux Liquid Scintillation Counter (PerkinElmer Life and Analytical Sciences, Waltham, MA).

Hot plate studies:

The hot-plate test is adapted from that described previously (Tyers, 1980). Male C57BL/6J mice (20-25g) or male Sprague-Dawley rats (200-250g) were acclimated to the vivarium for 48 hrs. Animals were placed individually on a heated surface (56°C for mice, 52°C for rats) and the time interval (seconds) between placement and a shaking, licking, or tucking of the hind paw was recorded as the predrug latency response. This same procedure was repeated 30 minutes after subcutaneous (s.c.) administration of compound in 10% ethanol, 10% cremophor, 80% water (10-10-80). All compounds were administered s.c. in a volume of 1 ml/100 g, with volume adjustments made for mouse dosing. The cutoff time,

JPET Fast Forward. Published on January 8, 2013 as DOI: 10.1124/jpet.112.201616
This article has not been copyedited and formatted. The final version may differ from this version.

designed to prevent injury to the animals, was 30 seconds (with vehicle latencies of approximately 5–10 seconds). The percent maximum possible antinociceptive effect (% MPE) was determined using the formula:

Percent MPE = ((Post drug latency – baseline latency) / (30 – baseline latency)) x 100 (1)

We used the pre-drug latency of each animal and cutoff times as noted above. Experimenter was blind to the treatment of animals during behavioral observations.

Rat tail flick studies:

The tail flick assay is adapted from the procedure originally described (D'Amour and Smith, 1941). In the present experiment, male Sprague-Dawley rats (200-250 grams) acclimated to the vivarium for 48 hours prior to behavioral testing. On the day of testing, animals were randomly assigned to vehicle (10-10-80, as before), TRV130, or morphine treatment groups. All compounds were administered s.c. in a volume of 1 ml/kg. Experimenter was blind to the treatment of animals during behavioral observations. Prior to drug treatment, each animal was tested to determine the baseline response. Rats were gently restrained using a towel and the distal third of the tail was placed on the tail flick apparatus (Columbus Instruments, Columbus Ohio), which was set at a temperature that would produce a consistent baseline response of 3-6 seconds. In this assay, the latency of the rat to withdraw the tail from the radiant thermal stimulus was recorded. After baseline testing, animals received a s.c. injection of vehicle or test compound. At 30 minutes post-drug, animals were re-tested. A cutoff time of 15 seconds was used to prevent injury to the animal. MPE was calculated as with hot plate.

Rat incisional pain studies:

Experiments were conducted in male Sprague-Dawley rats (200-250g). Animals acclimated to the vivarium for 48 hr prior to surgery. The measurement of tactile sensitivity for the injured hind paw was obtained using Von Frey filaments and the up/down method previously described (Dixon, 1980; LaBuda and Little, 2005). Twenty-four hours after surgery, animals were randomly assigned to vehicle, TRV130 or morphine treatment groups. All compounds were administered intravenously (i.v.) as a bolus in the rat

JPET Fast Forward. Published on January 8, 2013 as DOI: 10.1124/jpet.112.201616
This article has not been copyedited and formatted. The final version may differ from this version.

tail in a volume of 1 ml/kg (vehicle as before, 10-10-80). Allodynia was measured 30 minutes after drug administration.

Mouse GI function studies:

Glass bead colonic motility assay

Mice (C57BL/6J, 20-25g) were fasted overnight to afford an accurate measurement of colonic transit. Animals were allowed free access to water the night before the experiment. On the day of the experiment animals were weighed and compounds were administered as in the hot plate experiments 20 minutes before the insertion of a single 2 mm glass bead 2 cm into the distal colon of each mouse (Raehal et al., 2005). Time until bead expulsion was recorded with an assay maximum of 240 minutes (100% MPE).

Fecal boli assay

Mice (C57BL/6J, 20-25g) were allowed access to food and water ad libitum. On the day of the experiment, animals were weighed and compounds were administered s.c. (as in hot plate studies), 20 minutes after animals were placed individually in a testing chamber. Fecal boli were removed from each animal's test chamber and weighed hourly for four hours (Raehal et al., 2005). Because TRV130 had a weak effect in this assay, the Hill Slope was fixed to 1.0 to allow curve fitting to determine the ED_{50}. 100% MPE is defined in this assay as zero grams fecal boli production, and vehicle-treated animals define the 0% effect boundary.

Rat blood gas studies:

Briefly, respiratory suppression was determined using male Sprague-Dawley rats (200-250g) surgically prepared with carotid artery catheters. Animals were administered either vehicle, TRV130 at doses of 0.3, 0.6, 1.2 and 2.4 mg/kg s.c. or morphine 3, 6, 12 and 24 mg/kg, s.c. in a volume of 2ml/kg prepared in the same vehicle solution as was used as in the rat hot plate, tail-flick, and incisional pain assays. Arterial blood samples (approximately 0.5ml/sample) were collected from the arterial catheter from all animals at pre-dose, 5, 30, 120 and 240 minutes following dosing for pCO_2, pO_2 and pH measurement. Rats were observed for behavioral changes prior to dosing, and approximately 30 minutes, 2 and 4 hours post dose.

***Pharmacokinetics*:**

JPET Fast Forward. Published on January 8, 2013 as DOI: 10.1124/jpet.112.201616
This article has not been copyedited and formatted. The final version may differ from this version.

Plasma and brain levels of TRV130 were determined by ChemPartner (Shanghai, China) after i.v. or s.c. (10-10-80 vehicle) dosing of the species listed in Table 2 by standard mass spectrometry bioanalytical methods. Brain levels of TRV130 were measured in mice. Over an 8 hour period, samples were taken at 0, 7.5 min, 15 min, 30 min, 1hr, 2hr, 4hr, and 8hr in all species. Standard pharmacokinetic calculations were used to produce values in Table 2.

Quantification of ligand bias:

We applied an "equiactive comparison" between signaling pathways previously described (Griffin et al., 2007; Rajagopal et al., 2011). Estimates of the intrinsic relative activity (RAi) for both the G-protein (RAiG) or β-arrestin signaling (RAiBarr) pathways are calculated using equation 2. The bias ratio for efficacy of G-protein signaling versus β-arrestin is determined as the ratio of these intrinsic relative activities.

$$RAi = \frac{E_{max}\, ref \cdot EC_{50}\, lig}{E_{max}\, lig \cdot EC_{50}\, ref} \quad (2)$$

This method assumes that measured responses reflect ligand binding at equilibrium and that hill slopes are 1.0; both of these assumptions are supported by the data presented here. In addition, we used the "equimolar" comparison of compound responses at the same ligand concentrations for both G-protein and β-arrestin2 pathways to qualitatively demonstrate bias (Rajagopal et al., 2011).

***Statistics*:** Statistics were calculated using Prism version 5 (GraphPad Inc, San Diego, California). Compound ED_{50} values were determined using a computer-assisted non-linear regression analysis of the dose-response curve. We also measured one way analysis of variance (ANOVA) using GraphPad Prism with a Tukey-Kramer multiple comparison post-test (GraphPad Software, San Diego, CA).

Results

TRV130 is a G protein-biased ligand at the MOR

To identify G protein coupling biased ligands of the MOR, we screened Trevena's internal chemical library, measuring both G protein coupling (by inhibition of forskolin-stimulated cAMP

JPET Fast Forward. Published on January 8, 2013 as DOI: 10.1124/jpet.112.201616
This article has not been copyedited and formatted. The final version may differ from this version.

accumulation) and β-arrestin2 recruitment to the human MOR (by enzyme complementation). Several active compounds in a related chemical series were identified and further optimized for potency, ligand bias, and selectivity, resulting in the discovery of [(3-methoxythiophen-2-yl)methyl]({2-[(9R)-9-(pyridin-2-yl)-6-oxaspiro[4.5]decan-9-yl]ethyl}2)amine (TRV130; depicted in Figure 1). This compound shows no structural similarity to morphine, fentanyl, or other previously described MOR agonists.

In HEK cells, TRV130 displays G protein coupling efficacy comparable to morphine (71% and 92% respectively of the full agonist DAMGO) and higher potency than morphine (8 nM vs. 50 nM), but TRV130 displays approximately 14% of the efficacy of morphine for β-arrestin2 recruitment (Figure 2). Morphine itself is a partial agonist in the β-arrestin2 assay, as DAMGO has 8.8-fold higher efficacy and fentanyl has 4.8-fold higher efficacy than morphine (Supplemental Table 1). This is consistent with the potency and efficacy of morphine in a bioluminescence resonance energy transfer assay (Molinari et al., 2010). When we applied a mathematical model for the quantification of ligand bias, the ratio of intrinsic relative activities proposed by Ehlert and colleagues (Griffin et al., 2007) and later applied to G protein versus β-arrestin ligand bias (Rajagopal et al., 2011), we find TRV130 possesses approximately 3 fold preference for the G pathway over β-arrestin2 relative to morphine and fentanyl (Supplemental Table 2). The low β-arrestin2 efficacy of TRV130 leads to an uncertain EC_{50}, precluding a statistical comparison of this bias; however, bias is also reflected qualitatively in an "equimolar" comparison of G protein and β-arrestin responses for TRV130 and morphine (Supplemental Figure 6) (Rajagopal et al., 2011). Thus, TRV130 appears unique compared to widely used opioid analgesics: it is a strong agonist like morphine but fails to robustly engage β-arrestin2 recruitment. Similar in vitro results for the potencies and efficacies of TRV130 with respect to this set of compounds were observed in G protein and β-arrestin2 coupling assays for the mouse, rat, and dog MORs (Table 1). In addition TRV130 bound with high affinity to human, mouse and rat MOR species orthologs (Table 1).

In general, β-arrestins desensitize GPCRs to reduce G protein signaling while promoting receptor internalization and stimulating G-protein-independent signaling (DeWire and Violin, 2011). In accord

JPET Fast Forward. Published on January 8, 2013 as DOI: 10.1124/jpet.112.201616
This article has not been copyedited and formatted. The final version may differ from this version.

with its reduced efficacy for β-arrestin recruitment, TRV130 exhibited minimal receptor internalization in a highly sensitive enzyme complementation assay of receptor endocytosis (Figure 3A). Morphine caused significant internalization of the MOR in this assay, at a level of approximately 40% that of the maximal responses of fentanyl and DAMGO, consistent with modest ability of morphine to promote receptor internalization (Haberstock-Debic et al., 2005). Similarly, TRV130 caused significantly less receptor phosphorylation at serine 375 on the carboxy-terminal region of the MOR than did several other strong opioids (Figure 3B). This again is consistent with the lack of β-arrestin engagement by TRV130, since carboxy-terminal receptor phosphorylation is a major driver of β-arrestin coupling to receptor (Tohgo et al., 2003). Interestingly, morphine was a full agonist for the phosphorylation of this serine on the receptor, consistent with literature reports (Doll et al., 2011) and further supporting that compared to morphine, TRV130 selectively fails to engage the G protein coupled receptor kinase (GRK)/β-arrestin/receptor internalization axis of receptor function.

Naloxone shifted the EC_{50} of TRV130-evoked G protein coupling in a concentration-dependent manner consistent with a competitive mechanism of action (Figure 4A). Fitting the data to a modified Gaddum/Schild competitive interaction model (Lazareno and Birdsall, 1993; Lew and Angus, 1995) supported this conclusion. In the same manner, TRV130 competitively displaced the EC_{50} of DAMGO-stimulated β-arrestin2 recruitment (Figure 4B), again consistent with a competitive interaction and a binding site for TRV130 that is shared with classic opioid ligands. Consistent with this finding, kinetic radioligand binding studies revealed a residence time of approximately 2 minutes for TRV130 at the hMOR, which is similar to the residence times of morphine and fentanyl (Supplemental Table 3).

We also measured TRV130's activity at the human κ-opioid receptor (KOR), δ-opioid receptor (DOR), and nociceptin receptor (NOP) and found that the compound is remarkably selectivity for the MOR (Table 1). TRV130 is approximately 400 fold selective for the MOR over the KOR, DOR and NOP receptors in our cell based assays. In contrast, morphine is only 10 fold selective for the MOR over the KOR and DOR opioid subtypes. In addition to, TRV130 had more than 130- fold selectivity for the

JPET Fast Forward. Published on January 8, 2013 as DOI: 10.1124/jpet.112.201616
This article has not been copyedited and formatted. The final version may differ from this version.

MOR over human α_{2C}, D_{2S}, D_3, 5-HT_{1a} and σ receptors in radioligand displacement studies, and weak binding (defined as <50% inhibition of binding at 10 μM) to 120 other receptors, channels, and enzymes (Supplemental Table 4). Thus TRV130 is a potent, selective, and G protein-biased ligand of the MOR.

TRV130 is a rapid and powerful analgesic in rats and mice

To assess the analgesic activity of TRV130, we ran a battery of assays in rodents. First, TRV130 was compared to morphine for anti-nociceptive activity in the 56°C hot plate assay in mice, which is sensitive only to highly efficacious analgesics like strong opioids, and involves both spinal and supraspinal responses (Le Bars et al., 2001). TRV130 displays an ED_{50} of 0.9 mg/kg and morphine displays an ED_{50} of 4.9 mg /kg, with both compounds showing maximal efficacy in the assay (Figure 5A, Supplemental Table 5). TRV130 reached peak analgesia at 5 minutes compared to 30 minutes for morphine, but the duration of action for TRV130 and morphine were similar at approximately 90 minutes (Figure 5B). TRV130 analgesia was also reversible in mice by administration of 3 mg/kg naloxone s.c. 15 minutes after TRV130 dosing (Supplemental Figure 1), demonstrating that the observed analgesia is MOR-mediated, and also supported by the short residence time of TRV130 on the receptor (Supplemental Table 3). In rats, TRV130 was also robustly analgesic in several assays. In the rat 52 °C hot plate, TRV130 was 10-fold more potent than morphine (ED_{50}'s of 0.32 and 3.2 mg/kg, respectively) (Figure 6A, Supplemental Table 5). TRV130 showed similarly increased potency compared to morphine in the rat tail-flick model (Figure 6B, Supplemental Table 5) and rat hindpaw incisional pain model (Figure 6C).

These pharmacodynamic findings are consistent with the pharmacokinetics of TRV130, which shows rapid brain penetration (67% of plasma drug levels are achieved in brain samples, and peak brain exposure was observed at 15 minutes post dosing, data not shown) and an exposure time-course similar to the analgesic time-course (Table 2). The pharmacokinetics of TRV130 after intravenous bolus in a variety of preclinical species showed relatively high volumes of distribution and largely monophasic

JPET Fast Forward. Published on January 8, 2013 as DOI: 10.1124/jpet.112.201616
This article has not been copyedited and formatted. The final version may differ from this version.

clearance, similar to morphine (Table 2). This profile suggests TRV130 will be generally similar to medium-duration analgesics like morphine and hydromorphone, but with more rapid brain penetration consistent with the lipophilicity of TRV130, as reflected in LogP values (3.19 for TRV130 and 0.87 for morphine). Additionally, this profile suggests that TRV130 and morphine can be compared fairly in the rodent studies used here, some of which are time-sensitive. TRV130 showed extensive first pass metabolism and less than 6% oral availability in rats and mice (data not shown).

TRV130 possesses an improved therapeutic index of analgesia to constipation relative to morphine in mice

The impact of TRV130 and morphine on gastrointestinal function were evaluated in the mouse glass bead expulsion assay of colonic motility (Figure 7, blue curves, Supplemental Table 5) and fecal boli accumulation assay (Figure 7 orange curves, Supplemental Table 5). These responses were then compared to the hot-plate anti-nociceptive responses (Figure 7, black curves). These models show that TRV130 causes less gastrointestinal dysfunction than morphine at equivalent analgesic doses. This difference is best reflected in the lack of gastrointestinal dysfunction at the subanalgesic dose of 0.3 mg/kg s.c. of TRV130, compared to marked dysfunction caused by morphine at the similarly subanalgesic dose of 1 mg/kg s.c. Similarly, at maximally analgesic doses of TRV130, colonic motility was still evident, whereas morphine at equivalently analgesic doses completely blocked gastrointestinal function (100% MPE). A similar improvement in GI function was noted in the fecal boli accumulation assay (Figure 7, orange curves) and the charcoal meal gastrointestinal transit test (Supplemental Figure 2). Together, these data suggest that TRV130 may cause less opioid-induced constipation than morphine.

TRV130 shows an improved therapeutic index of analgesia to respiratory suppression compared to morphine in rats

Rats were used to compare TRV130 and morphine with respect to analgesia and respiratory suppression, because the larger blood volume of rats makes serial arterial blood gas measurement more

JPET Fast Forward. Published on January 8, 2013 as DOI: 10.1124/jpet.112.201616
This article has not been copyedited and formatted. The final version may differ from this version.

feasible than in mice (Sahbaie et al., 2006). The equianalgesic doses of 3.0 mg/kg morphine and 0.3 mg/kg TRV130 were chosen, based on responses in the rat hot-plate (Figure 6A), tail flick (Figure 6B), and hindpaw incision (Figure 6C), as a basis for comparing respiratory suppression at analgesic and supra-analgesic doses. Morphine caused a trend towards increasing pCO_2 at 3.0 and 6.0 mg/kg (Figures 8A and B), and caused a statistically significant increase in pCO_2 (greater than 50 mmHg, compared to 35-40 mmHg at baseline and in vehicle-treated animals) at doses 4-fold and 8-fold over the hot-plate ED_{50} (12 and 24 mg/kg) (Figures 8C and D). In contrast, TRV130 did not cause this severe level of respiratory suppression even at 8-fold over the equianalgesic dose (Figures 8C and 8D). This improved therapeutic index compared to the analgesic response is illustrated in Figure 8E and 8F as hot plate responses (in black) and peak pCO2 measurements (in orange); hot plate response was chosen for this comparison as it, like respiratory depression, involves supraspinal processing. pO_2 and pH measures largely paralleled the changes seen in pCO_2 for both morphine and TRV130 (Supplemental Figure 3). Behavioral notes during this study indicate that TRV130 was not nearly as sedative as morphine at equianalgesic doses, consistent with less CNS depression (Supplemental Figure 4). These findings indicate that in rats, TRV130 has an increased therapeutic index for analgesia vs. respiratory suppression and sedation.

Discussion

The data presented here demonstrate that TRV130 is a novel MOR G protein biased ligand. The unique in vitro and in vivo profile of TRV130 suggests that it may be possible to minimize on-target MOR-mediated adverse events, which could significantly improve opioid pain management. Furthermore, the recapitulation of morphine's improved pharmacology in β-arrestin2 KO mice by a ligand with reduced ability to engage β-arrestin2 demonstrates that molecular dissection of receptor signaling pathways can translate to differentiated pharmacology of biased ligands. Mechanistically, this could be the result of either a) reduced stimulation of an active, constipating and respiratory-suppressing signaling mechanism of β-arrestin, or b) selective amplification of the analgesic pathway, which may be more sensitive to the acute desensitization effects of β-arrestin than the respiratory or constipating signals. The

JPET Fast Forward. Published on January 8, 2013 as DOI: 10.1124/jpet.112.201616
This article has not been copyedited and formatted. The final version may differ from this version.

former mechanism is supported by the reduced impact of morphine on gastrointestinal motility and respiration in β-arrestin2 knockout mice compared to wild type mice (Raehal et al., 2005); the latter mechanism is supported by the increased anti-nociceptive efficacy of morphine in β-arrestin2 knockout mice compared to wild-type mice (Bohn et al., 1999). However, either mechanism could explain the observed improved therapeutic index for TRV130, and neither pharmacokinetics nor receptor selectivity seem likely contributors. At the molecular level, MOR G protein coupling leads to analgesia by activation of potassium channels and inhibition of calcium channels (Altier and Zamponi, 2004; Ocana et al., 2004), but further work will be required to clarify the specific intracellular signaling pathways downstream of β-arrestins that contribute to opioid responses in vivo. In addition, the recently published MOR crystal structure may permit investigation of how biased and unbiased ligands may engage different conformations of the MOR to support selective coupling to G proteins vs. β-arrestins (Manglik et al., 2012).

TRV130 shows a differentiated profile compared to morphine in several cellular readouts including β-arrestin2 recruitment, receptor phosphorylation, and receptor internalization. Morphine effects on these endpoints can be difficult to measure in low-sensitivity assays (Whistler and von Zastrow, 1998; Sternini et al., 2000), which sometimes require overexpressed GRK to amplify signal (Groer et al., 2007), but is clearly detectable in the more sensitive assays used here. The fact that morphine pharmacology is altered in β-arrestin2 KO mice, despite no apparent changes in baseline function, suggests that β-arrestin2 engagement by morphine is meaningful, and that the more sensitive in vitro assays are measuring relevant molecular pharmacology, even if morphine is a partial agonist with respect to higher efficacy drugs such as fentanyl. Importantly, morphine is not biased with respect to fentanyl in the model used here, whereas TRV130 is biased with respect to both fentanyl and morphine. This suggests that despite higher efficacy of fentanyl than morphine for both G protein and β-arrestin responses, morphine and fentanyl, unlike TRV130, do not display functional selectivity for β-arrestin engagement at equi-active concentrations.

JPET Fast Forward. Published on January 8, 2013 as DOI: 10.1124/jpet.112.201616
This article has not been copyedited and formatted. The final version may differ from this version.

Quantification of ligand bias is particularly useful in systems such as overexpressed MOR where one pathway may be selectively amplified such that partial agonists appear as biased ligands. Here we have used "equiactive comparison" approach (Griffin et al., 2007; Rajagopal et al., 2011), which calculates intrinsic relative activity for each downstream pathway. The model we used assumes that ligands are signaling from a state of equilibrium binding, and that dose-response curves show no cooperativity; the data presented here indicates that both of these assumptions appear reasonable for TRV130, morphine, and fentanyl. By this calculation, TRV130 is approximately 3 fold more biased towards G protein signaling than morphine and fentanyl (Supplemental Table 2).

The profile of TRV130 both in vitro and in vivo is inconsistent with functional selectivity arising from unbiased partial efficacy. In our assays, TRV130 shows robust, morphine-like G protein coupling, with efficacy of 83% of morphine, whereas the well-described partial agonist buprenorphine displays efficacy of only 52% of morphine (Supplemental Table 1). In vivo, buprenorphine behaves as a partial agonist in both the analgesia and colonic motility assays (Supplemental Figure 5), except with more glass bead retention than analgesia. Morphine exhibits full efficacy in each of these two in vivo assays, and TRV130 has maximal efficacy for analgesia but only partial efficacy in the colonic motility and fecal production assays. This highlights the differentiation of TRV130 as a biased ligand from both a strong agonist and a partial agonist, and suggests that the functional selectivity of TRV130 in vivo does not arise from differential amplification of partial agonist signals.

The profile of TRV130 shown here, of robust analgesia with reduced CNS depression and reduced gastrointestinal dysfunction compared to morphine, should translate into an important improvement in the treatment of post-operative pain. In this setting, post-operative nausea and vomiting, constipation, and sedation caused by current opioids cause significant patient discomfort and can prolong hospital stay. The risk of respiratory suppression limits opioid dosing, leaving many patients in pain during recuperation (Dahan, 2007). Thus TRV130 may be a marked improvement over current opioids in post-operative care. These improvements could also hold great promise for chronic pain management,

JPET Fast Forward. Published on January 8, 2013 as DOI: 10.1124/jpet.112.201616
This article has not been copyedited and formatted. The final version may differ from this version.

where constipation is a severe and often dose-limiting adverse event (Anastassopoulos et al., 2011). Chronic opioid use also increases the risk of opioid addiction and tolerance to the analgesic benefits (Schneider and Kirsh, 2010). While these facets of MOR pharmacology will be explored with TRV130 in future studies, several of the previous studies of morphine in β-arrestin2 knockout mice suggest that TRV130 may have reduced potential for addiction and analgesic tolerance (Bohn et al., 2000; Bohn et al., 2003; Raehal and Bohn, 2011; Urs et al., 2011).

Based on the preclinical profile described here, TRV130 is now in clinical development for use as an intravenous analgesic alternative to morphine and fentanyl. Although rodent oral bioavailability of TRV130 is low, the potential for oral availability in higher species is still being explored. Based on preliminary data suggesting high skin permeation, TRV130 is also being investigated for administration via a transdermal patch to treat chronic pain. If the differentiation versus morphine shown here successfully translates to humans, the improved therapeutic windows of analgesia to respiratory suppression and gastrointestinal effects could provide physicians a more tolerable analgesic with a higher margin of safety. This in turn would lead to more effective pain management. More broadly, this would represent the successful translation of selective signaling via ligand bias to improve the therapeutic profile of a GPCR-targeted drug. In turn, this strategy could be applied to other GPCRs for which on-target adverse events limit therapeutic utility.

Acknowledgments

We are grateful to Ian James for critical reading of this manuscript.

Participated in research design: DeWire, Rominger,Violin, Yamashita, Cowan, Lark, Koblish, Graczyk.
Conducted experiments: DeWire, Rominger, Koblish, Graczyk.
Contributed new reagents or analytic tools: Liu, Chen, Gotchev, Pitis, Yuan, Yamashita.
Performed data analysis: DeWire, Cowan, Rominger, Violin.
Wrote or contributed to the writing of the manuscript: DeWire, Rominger, Violin, Cowan, Yamashita, Lark.

References

Allen JA, Yost JM, Setola V, Chen X, Sassano MF, Chen M, Peterson S, Yadav PN, Huang XP, Feng B, Jensen NH, Che X, Bai X, Frye SV, Wetsel WC, Caron MG, Javitch JA, Roth BL and Jin J (2011) Discovery of beta-arrestin-biased dopamine D2 ligands for probing signal transduction pathways essential for antipsychotic efficacy. *Proc Natl Acad Sci U S A* **108**:18488-18493.

Altier C and Zamponi GW (2004) Targeting Ca2+ channels to treat pain: T-type versus N-type. *Trends Pharmacol Sci* **25**:465-470.

Anastassopoulos KP, Chow W, Ackerman SJ, Tapia C, Benson C and Kim MS (2011) Oxycodone-related side effects: impact on degree of bother, adherence, pain relief, satisfaction, and quality of life. *J Opioid Manag* **7**:203-215.

Audet N, Charfi I, Mnie-Filali O, Amraei M, Chabot-Dore AJ, Millecamps M, Stone LS and Pineyro G (2012) Differential association of receptor-Gbetagamma complexes with beta-arrestin2 determines recycling bias and potential for tolerance of delta opioid receptor agonists. *J Neurosci* **32**:4827-4840.

Azzi M, Charest PG, Angers S, Rousseau G, Kohout T, Bouvier M and Pineyro G (2003) Beta-arrestin-mediated activation of MAPK by inverse agonists reveals distinct active conformations for G protein-coupled receptors. *Proc Natl Acad Sci U S A* **100**:11406-11411.

Bohn LM, Gainetdinov RR, Lin FT, Lefkowitz RJ and Caron MG (2000) Mu-opioid receptor desensitization by beta-arrestin-2 determines morphine tolerance but not dependence. *Nature* **408**:720-723.

Bohn LM, Gainetdinov RR, Sotnikova TD, Medvedev IO, Lefkowitz RJ, Dykstra LA and Caron MG (2003) Enhanced rewarding properties of morphine, but not cocaine, in beta(arrestin)-2 knock-out mice. *J Neurosci* **23**:10265-10273.

Bohn LM, Lefkowitz RJ, Gainetdinov RR, Peppel K, Caron MG and Lin FT (1999) Enhanced morphine analgesia in mice lacking beta-arrestin 2. *Science* **286**:2495-2498.

Bostrom BM, Ramberg T, Davis BD and Fridlund B (1997) Survey of post-operative patients' pain management. *J Nurs Manag* **5**:341-349.

D'Amour FE and Smith DL (1941) A method for determining loss of pain sensation. *Journal of Pharmacology and Experimental Therapeutics* **72**:74-79.

Dahan A (2007) Respiratory depression with opioids. *J Pain Palliat Care Pharmacother* **21**:63-66.

DeWire SM, Ahn S, Lefkowitz RJ and Shenoy SK (2007) Beta-arrestins and cell signaling. *Annu Rev Physiol* **69**:483-510.

DeWire SM and Violin JD (2011) Biased ligands for better cardiovascular drugs: dissecting G-protein-coupled receptor pharmacology. *Circ Res* **109**:205-216.

Dixon WJ (1980) Efficient Analysis of Experimental Observations. *Annual Review of Pharmacology and Toxicology* **20**:441-462.

Doll C, Konietzko J, Poll F, Koch T, Hollt V and Schulz S (2011) Agonist-selective patterns of micro-opioid receptor phosphorylation revealed by phosphosite-specific antibodies. *Br J Pharmacol* **164**:298-307.

Eason MG, Jacinto MT and Liggett SB (1994) Contribution of ligand structure to activation of alpha 2-adrenergic receptor subtype coupling to Gs. *Mol Pharmacol* **45**:696-702.

Gesty-Palmer D, Chen M, Reiter E, Ahn S, Nelson CD, Wang S, Eckhardt AE, Cowan CL, Spurney RF, Luttrell LM and Lefkowitz RJ (2006) Distinct beta-arrestin- and G protein-dependent pathways for parathyroid hormone receptor-stimulated ERK1/2 activation. *J Biol Chem* **281**:10856-10864.

Gesty-Palmer D, Flannery P, Yuan L, Corsino L, Spurney R, Lefkowitz RJ and Luttrell LM (2009) A beta-arrestin-biased agonist of the parathyroid hormone receptor (PTH1R) promotes bone formation independent of G protein activation. *Sci Transl Med* **1**:1ra1.

Gesty-Palmer D and Luttrell LM (2011) Refining efficacy: exploiting functional selectivity for drug discovery. *Adv Pharmacol* **62**:79-107.

Griffin MT, Figueroa KW, Liller S and Ehlert FJ (2007) Estimation of agonist activity at G protein-coupled receptors: analysis of M2 muscarinic receptor signaling through Gi/o,Gs, and G15. *J Pharmacol Exp Ther* **321**:1193-1207.

Groer CE, Tidgewell K, Moyer RA, Harding WW, Rothman RB, Prisinzano TE and Bohn LM (2007) An opioid agonist that does not induce mu-opioid receptor--arrestin interactions or receptor internalization. *Mol Pharmacol* **71**:549-557.

Haberstock-Debic H, Kim KA, Yu YJ and von Zastrow M (2005) Morphine promotes rapid, arrestin-dependent endocytosis of mu-opioid receptors in striatal neurons. *J Neurosci* **25**:7847-7857.

Hamilton GR and Baskett TF (2000) In the arms of Morpheus the development of morphine for postoperative pain relief. *Can J Anaesth* **47**:367-374.

Kenakin T (2011) Functional selectivity and biased receptor signaling. *J Pharmacol Exp Ther* **336**:296-302.

Kieffer BL (1999) Opioids: first lessons from knockout mice. *Trends Pharmacol Sci* **20**:19-26.

Kim IM, Tilley DG, Chen J, Salazar NC, Whalen EJ, Violin JD and Rockman HA (2008) Beta-blockers alprenolol and carvedilol stimulate beta-arrestin-mediated EGFR transactivation. *Proc Natl Acad Sci U S A* **105**:14555-14560.

LaBuda CJ and Little PJ (2005) Pharmacological evaluation of the selective spinal nerve ligation model of neuropathic pain in the rat. *Journal of Neuroscience Methods* **144**:175-181.

Lazareno S and Birdsall NJ (1993) Estimation of competitive antagonist affinity from functional inhibition curves using the Gaddum, Schild and Cheng-Prusoff equations. *Br J Pharmacol* **109**:1110-1119.

Le Bars D, Gozariu M and Cadden SW (2001) Animal models of nociception. *Pharmacol Rev* **53**:597-652.

Lew MJ and Angus JA (1995) Analysis of competitive agonist-antagonist interactions by nonlinear regression. *Trends Pharmacol Sci* **16**:328-337.

Li Y, Liu X, Liu C, Kang J, Yang J, Pei G and Wu C (2009) Improvement of morphine-mediated analgesia by inhibition of beta-arrestin 2 expression in mice periaqueductal gray matter. *Int J Mol Sci* **10**:954-963.

Ma L, Seager MA, Wittmann M, Jacobson M, Bickel D, Burno M, Jones K, Graufelds VK, Xu G, Pearson M, McCampbell A, Gaspar R, Shughrue P, Danziger A, Regan C, Flick R, Pascarella D, Garson S, Doran S, Kreatsoulas C, Veng L, Lindsley CW, Shipe W, Kuduk S, Sur C, Kinney G, Seabrook GR and Ray WJ (2009) Selective activation of the M1 muscarinic acetylcholine receptor achieved by allosteric potentiation. *Proc Natl Acad Sci U S A* **106**:15950-15955.

Manchikanti L, Helm S, 2nd, Fellows B, Janata JW, Pampati V, Grider JS and Boswell MV (2012) Opioid epidemic in the United States. *Pain Physician* **15**:ES9-38.

Manglik A, Kruse AC, Kobilka TS, Thian FS, Mathiesen JM, Sunahara RK, Pardo L, Weis WI, Kobilka BK and Granier S (2012) Crystal structure of the micro-opioid receptor bound to a morphinan antagonist. *Nature* **485**:321-326.

Marderstein EL and Delaney CP (2008) Management of postoperative ileus: focus on alvimopan. *Ther Clin Risk Manag* **4**:965-973.

Matthes HW, Maldonado R, Simonin F, Valverde O, Slowe S, Kitchen I, Befort K, Dierich A, Le Meur M, Dolle P, Tzavara E, Hanoune J, Roques BP and Kieffer BL (1996) Loss of morphine-induced analgesia, reward effect and withdrawal symptoms in mice lacking the mu-opioid-receptor gene. *Nature* **383**:819-823.

Molinari P, Vezzi V, Sbraccia M, Gro C, Riitano D, Ambrosio C, Casella I and Costa T (2010) Morphine-like opiates selectively antagonize receptor-arrestin interactions. *J Biol Chem* **285**:12522-12535.

Ocana M, Cendan CM, Cobos EJ, Entrena JM and Baeyens JM (2004) Potassium channels and pain: present realities and future opportunities. *Eur J Pharmacol* **500**:203-219.

Raehal KM and Bohn LM (2011) The role of beta-arrestin2 in the severity of antinociceptive tolerance and physical dependence induced by different opioid pain therapeutics. *Neuropharmacology* **60**:58-65.

Raehal KM, Walker JK and Bohn LM (2005) Morphine side effects in beta-arrestin 2 knockout mice. *J Pharmacol Exp Ther* **314**:1195-1201.

Rajagopal K, Whalen EJ, Violin JD, Stiber JA, Rosenberg PB, Premont RT, Coffman TM, Rockman HA and Lefkowitz RJ (2006) Beta-arrestin2-mediated inotropic effects of the angiotensin II type 1A receptor in isolated cardiac myocytes. *Proc Natl Acad Sci U S A* **103**:16284-16289.

Rajagopal S, Ahn S, Rominger DH, Gowen-MacDonald W, Lam CM, Dewire SM, Violin JD and Lefkowitz RJ (2011) Quantifying ligand bias at seven-transmembrane receptors. *Mol Pharmacol* **80**:367-377.

Rosethorne EM and Charlton SJ (2011) Agonist-biased signaling at the histamine H4 receptor: JNJ7777120 recruits beta-arrestin without activating G proteins. *Mol Pharmacol* **79**:749-757.

Sahbaie P, Modanlou S, Gharagozlou P, Clark JD, Lameh J and Delorey TM (2006) Transcutaneous blood gas CO2 monitoring of induced ventilatory depression in mice. *Anesth Analg* **103**:620-625.

Schneider JP and Kirsh KL (2010) Defining clinical issues around tolerance, hyperalgesia, and addiction: a quantitative and qualitative outcome study of long-term opioid dosing in a chronic pain practice. *J Opioid Manag* **6**:385-395.

Sora I, Takahashi N, Funada M, Ujike H, Revay RS, Donovan DM, Miner LL and Uhl GR (1997) Opiate receptor knockout mice define mu receptor roles in endogenous nociceptive responses and morphine-induced analgesia. *Proc Natl Acad Sci U S A* **94**:1544-1549.

Spengler D, Waeber C, Pantaloni C, Holsboer F, Bockaert J, Seeburg PH and Journot L (1993) Differential signal transduction by five splice variants of the PACAP receptor. *Nature* **365**:170-175.

Sternini C, Brecha NC, Minnis J, D'Agostino G, Balestra B, Fiori E and Tonini M (2000) Role of agonist-dependent receptor internalization in the regulation of mu opioid receptors. *Neuroscience* **98**:233-241.

Tohgo A, Choy EW, Gesty-Palmer D, Pierce KL, Laporte S, Oakley RH, Caron MG, Lefkowitz RJ and Luttrell LM (2003) The stability of the G protein-coupled receptor-beta-arrestin interaction determines the mechanism and functional consequence of ERK activation. *J Biol Chem* **278**:6258-6267.

Tyers MB (1980) A classification of opiate receptors that mediate antinociception in animals. *Br J Pharmacol* **69**:503-512.

Urs NM, Daigle TL and Caron MG (2011) A dopamine D1 receptor-dependent beta-arrestin signaling complex potentially regulates morphine-induced psychomotor activation but not reward in mice. *Neuropsychopharmacology* **36**:551-558.

Violin JD, DeWire SM, Yamashita D, Rominger DH, Nguyen L, Schiller K, Whalen EJ, Gowen M and Lark MW (2010) Selectively engaging beta-arrestins at the angiotensin II type 1 receptor reduces blood pressure and increases cardiac performance. *J Pharmacol Exp Ther* **335**:572-579.

Violin JD and Lefkowitz RJ (2007) Beta-arrestin-biased ligands at seven-transmembrane receptors. *Trends Pharmacol Sci* **28**:416-422.

Wei H, Ahn S, Shenoy SK, Karnik SS, Hunyady L, Luttrell LM and Lefkowitz RJ (2003) Independent beta-arrestin 2 and G protein-mediated pathways for angiotensin II activation of extracellular signal-regulated kinases 1 and 2. *Proc Natl Acad Sci U S A* **100**:10782-10787.

Whistler JL and von Zastrow M (1998) Morphine-activated opioid receptors elude desensitization by beta-arrestin. *Proc Natl Acad Sci U S A* **95**:9914-9919.

Yang CH, Huang HW, Chen KH, Chen YS, Sheen-Chen SM and Lin CR (2011) Antinociceptive potentiation and attenuation of tolerance by intrathecal beta-arrestin 2 small interfering RNA in rats. *Br J Anaesth* **107**:774-781.

JPET Fast Forward. Published on January 8, 2013 as DOI: 10.1124/jpet.112.201616
This article has not been copyedited and formatted. The final version may differ from this version.

Footnotes

All work was funded by Trevena Inc. All authors are present or former employees of Trevena Inc, a privately held drug discovery company.

Reprint Requests

Jonathan Violin, Trevena Inc, 1018 West 8th Ave, Suite A, King of Prussia PA 19406.

Phone: 610-354-8840; Fax: 610-354-8850; email: jviolin@trevenainc.com

JPET Fast Forward. Published on January 8, 2013 as DOI: 10.1124/jpet.112.201616
This article has not been copyedited and formatted. The final version may differ from this version.

Legends for Figures

Figure 1. Chemical structure for TRV130 ([(3-methoxythiophen-2-yl)methyl]({2-[(9R)-9-(pyridin-2-yl)-6-oxaspiro[4.5]decan-9-yl]ethyl})amine), a novel MOR G protein-biased ligand.

Figure 2. TRV130 is a potent G-biased ligand at the hMOR. Compared to morphine (**A**) TRV130 (**B**) exhibits similar G protein coupling efficacy to morphine with reduced β-arrestin2 recruitment. β-arrestin2 recruitment was measured by chemiluminescent β-galactosidase activity (black), and G protein coupling was measured by inhibition of cAMP accumulation (orange), in HEK cells expressing human MOR. Data are means +/- standard error, displayed as percentage of maximum morphine efficacy, for greater than 30 independent experiments.

Figure 3. TRV130 exhibits reduced MOR internalization and phosphorylation. Compared to morphine, TRV130 exhibits (**A**) reduced receptor internalization (in an enzyme complementation assay) and (**B**) reduced MOR phosphorylation at serine 375. Equal protein amounts were loaded into each lane. For quantification, optical densities of total hMOR (S375) immunoreactive bands were measured, normalized to the background values, and expressed as percentages of controls. *, $P < 0.05$ vs vehicle; †, $P < 0.05$ vs morphine and data are means ± standard errors of 2-5 independent experiments.

Figure 4. TRV130 competitively binds the hMOR. A) Levels of cAMP inhibition were monitored after 30-min incubation with indicated concentrations of TRV130 and naloxone. Naloxone competitively shifted the cAMP inhibition curve for TRV130. (Schild slope = 0.9 ± 0.07), with an apparent K_B for naloxone of 6.6 nM. **B)** Levels of β-arrestin2 recruitment were monitored after 30-min incubation with indicated concentrations of DAMGO and TRV130. TRV130 competitively shifted DAMGO-induced β-arrestin2 recruitment (Schild slope = 1.2 ± 0.3 and an apparent K_B = 20 nM). Insets A and B, data were used to calculate dose ratios and K_B values for naloxone and TRV130. The graphs are representative of 2-5 independent experiments performed in duplicate.

JPET Fast Forward. Published on January 8, 2013 as DOI: 10.1124/jpet.112.201616
This article has not been copyedited and formatted. The final version may differ from this version.

Figure 5. TRV130 causes rapid analgesia in mice. A) Mice were injected s.c. with either TRV130 (orange circles) or morphine (blue squares) at the indicated doses, and 30 minutes later were subjected to a 56°C hot plate assay. The % of maximum possible effect was based on a 30 second assay cutoff. * indicates $p<0.05$ compared to vehicle-treated animals. **B)** Time course of TRV130 (1 mg/kg s.c.) and morphine (6 mg/kg, s.c.) analgesia in the 56°C hot plate. Mice were injected s.c. with either TRV130 or morphine, and 5, 15, 30, 60, and 90 minutes later were subjected to a 56°C hot plate assay. Data are mean ± standard errors of 4-14 animals per group.

Figure 6. TRV130 is analgesic in rats. A) Rats were injected s.c. with either TRV130 (orange bars) or morphine (blue bars) at the indicated doses, and 30 minutes later were subjected to a 52°C hot plate assay. The % of maximum possible effect was based on a 30 second assay cutoff. **B)** Rat tail flick latencies were performed for TRV130 and morphine at indicated doses. Percent of maximum response (15 second cutoff) is plotted. **C)** TRV130 and morphine are active in the rat hindpaw incisional pain model. Assay performed as described in the methods, to generate incisional allodynia. Rats were injected i.v. with TRV130 or morphine at the indicated doses. Von Frey fiber pressure measurements are plotted on the Y axis. * indicates $p<0.05$ compared to vehicle-treated animals. Data are mean ± standard errors of 4-14 animals per group.

Figure 7. TRV130 causes less gastrointestinal dysfunction than morphine in mice. Mice were injected s.c. with either morphine (A) or TRV130 (B) at the indicated doses, and 30 minutes later were subjected to either a 56°C hot plate (black curves, as in Figure 5), a glass bead colonic motility assay (blue curves), or a 4 hour fecal boli accumulation assay (orange curves). The % of maximum possible effect was based on 30 seconds in the hot plate, the cutoff time of 4 hours of bead retention in the glass bead assay, and no fecal production over 4 hours. Data are mean ± standard errors of 4-12 animals per group.

Figure 8. TRV130 exhibits less respiratory suppression than morphine in rats. A-D) Rats were injected s.c. with equianalgesic doses (and 2, 4, and 8 fold multiples of the ED_{50} doses) of TRV130 or morphine, and blood gas parameters including pCO_2, pO_2, and pH were monitored over a period of 4

JPET Fast Forward. Published on January 8, 2013 as DOI: 10.1124/jpet.112.201616
This article has not been copyedited and formatted. The final version may differ from this version.

hours. pCO_2 values are shown; pO_2 and pH are shown in supplemental Figure 3. **E-F)** Rats were injected s.c. with the indicated doses of TRV130 or morphine and subjected to a 52°C hot plate test (as in Figure 6A). Percent of maximum possible effect (30 second cutoff) in the hot plate for each dose is plotted against the left Y axis. In orange, the peak pCO_2 measurements for various doses from the experiment in A are plotted against the right Y axis to compare the analgesic and respiratory effects of these two compounds. Data are mean ± standard errors with n= 6 animals per group.

JPET Fast Forward. Published on January 8, 2013 as DOI: 10.1124/jpet.112.201616
This article has not been copyedited and formatted. The final version may differ from this version.

Table 1. MOR functional and binding specificity for TRV130

TRV130	cAMP				β-arrestin2				[^{3}H]diprenorphine	
	pEC_{50}	**SD**	**EC_{50} (nM)**	**Efficacy (%)**	**pEC_{50}**	**SD**	**EC_{50} (nM)**	**Efficacy (%)**	**$K_{i\ high}$ (nM)**	**$K_{i\ low}$ (nM)**
hMOR	8.1	0.04	7.9	83	7.4	0.22	40.0	14	6 ± 1.7	551 ± 263
mMOR	9.4	0.06	0.4	104	7.9	0.06	12.6	74	1 ± 0.3	39 ± 21
rMOR	8.4	0.03	4.0	90			N.Q.		18 ± 3.7	203 ± 26
dMOR	8.3	0.01	5.0	92	8.0	0.02	9.4	24	N.D.	
hNOP	6.4	0.09	398	58			N.Q.		N.D.	
hKOR	5.8	0.03	1585	58			N.Q.		>10,000	
hDOR	5.5	0.04	3162	46			N.Q.		N.D.	

Potencies and efficacies were determined for the indicated mu-opioid receptor (MOR) species orthologues
Efficacy values are calculated as % maximal response to morphine (h,r,m,d MOR), U69,593 (hKOR) and DPDPE (hDOR)
(n >10 independent experiments performed in duplicate) except dMOR n=3
$K_{i\ high}$ and $K_{i\ low}$ represent the high- and low-affinity binding component, respectively (n= 2-5 independent determinations)
N.Q. is not quantifiable N.D. is not determined

JPET Fast Forward. Published on January 8, 2013 as DOI: 10.1124/jpet.112.201616
This article has not been copyedited and formatted. The final version may differ from this version.

Table 2. Pharmacokinetics of TRV130 (i.v.) in mice, rats, dogs, and cynomolgous monkeys

Species	Dose (mg/kg)	AUC_{LAST} (hr•ng/mL)	terminal half-life $t_{1/2}$ (hr)	Clearance (L/kg/hr)	Vss (L/kg)
Mouse	0.3	35.9	2.45	8.27	4.5
Rat	0.5	70.8	0.8	6.97	6.9
Dog	0.5	992	3	0.64	0.51
Monkey	0.3	165	4.5	1.81	2.86

Figure 1

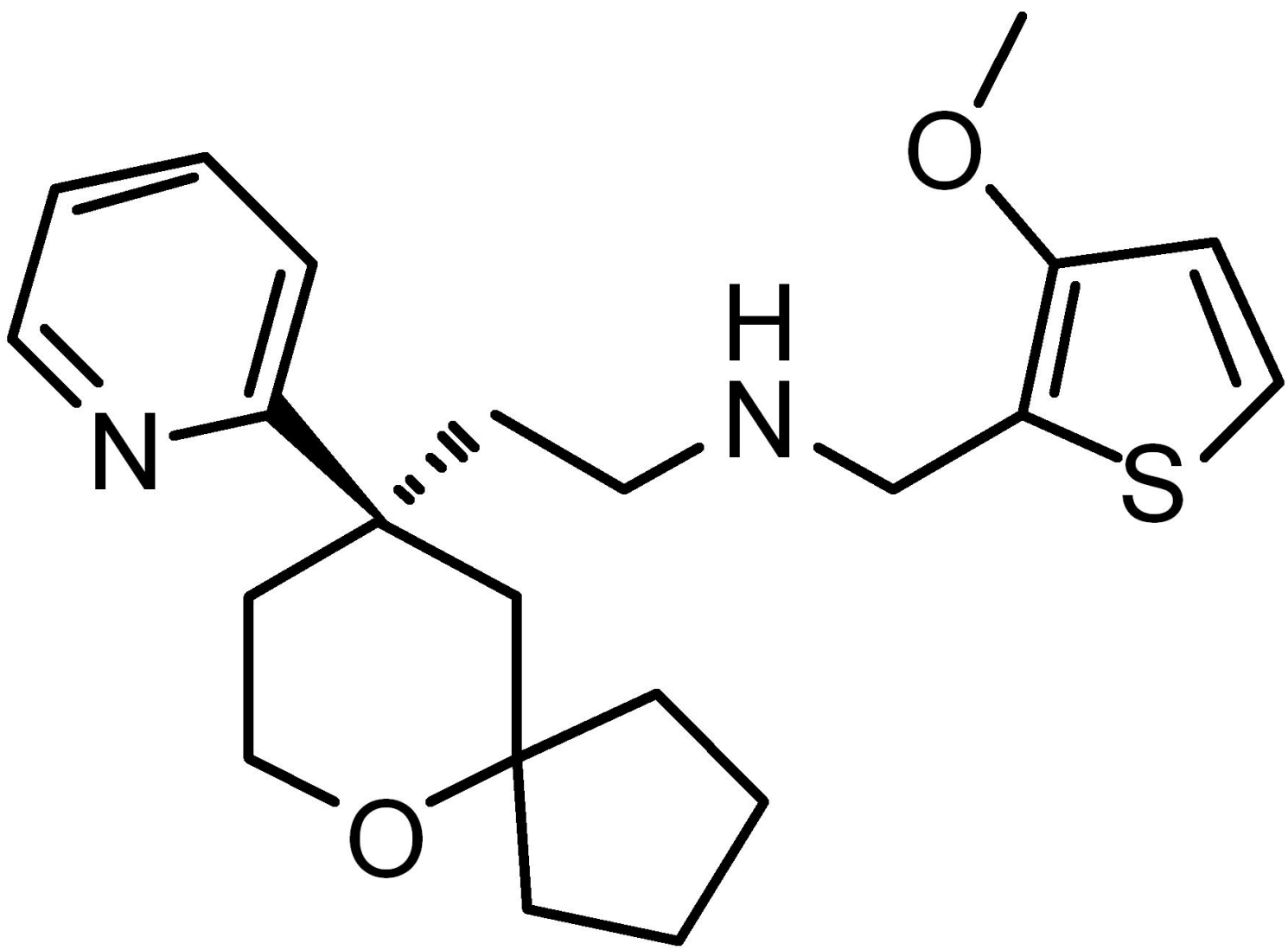

Figure 2

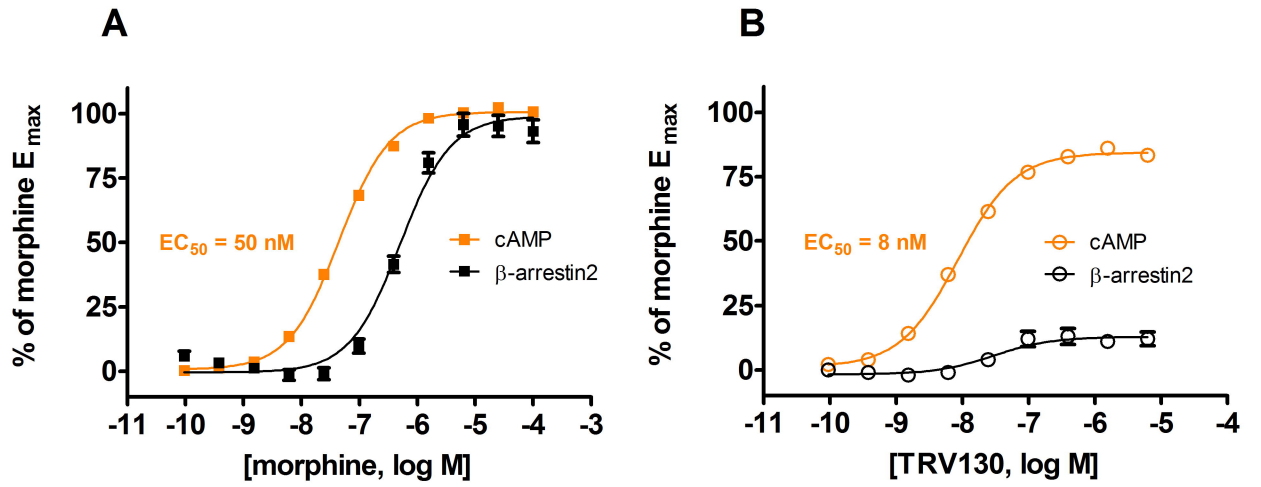
A
% of morphine E max
100
75
50
25
0
EC50 = 50 nM
cAMP
β-arrestin2
-11 -10 -9 -8 -7 -6 -5 -4 -3
[morphine, log M]
B
% of morphine E max
100
75
50
25
0
EC50 = 8 nM
cAMP
β-arrestin2
-11 -10 -9 -8 -7 -6 -5 -4
[TRV130, log M]

Figure 3

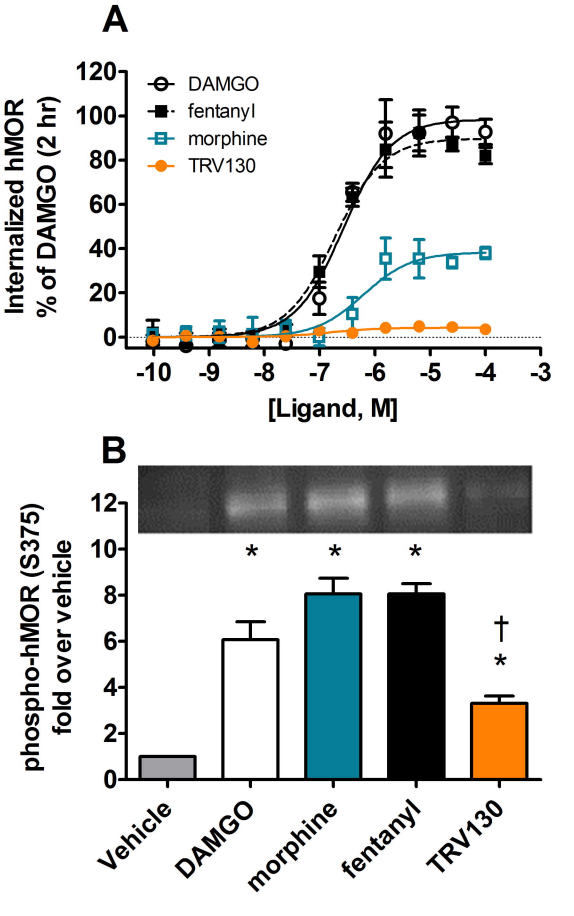
A
Internalized hMOR
% of DAMGO (2 hr)
120
100
80
60
40
20
0
DAMGO
fentanyl
morphine
TRV130
-10
-9
-8
-7
-6
-5
-4
-3
[Ligand, M]
B
phospho-hMOR (S375)
fold over vehicle
12
10
8
6
4
2
0
*
*
*
†
*
Vehicle
DAMGO
morphine
fentanyl
TRV130

Figure 4

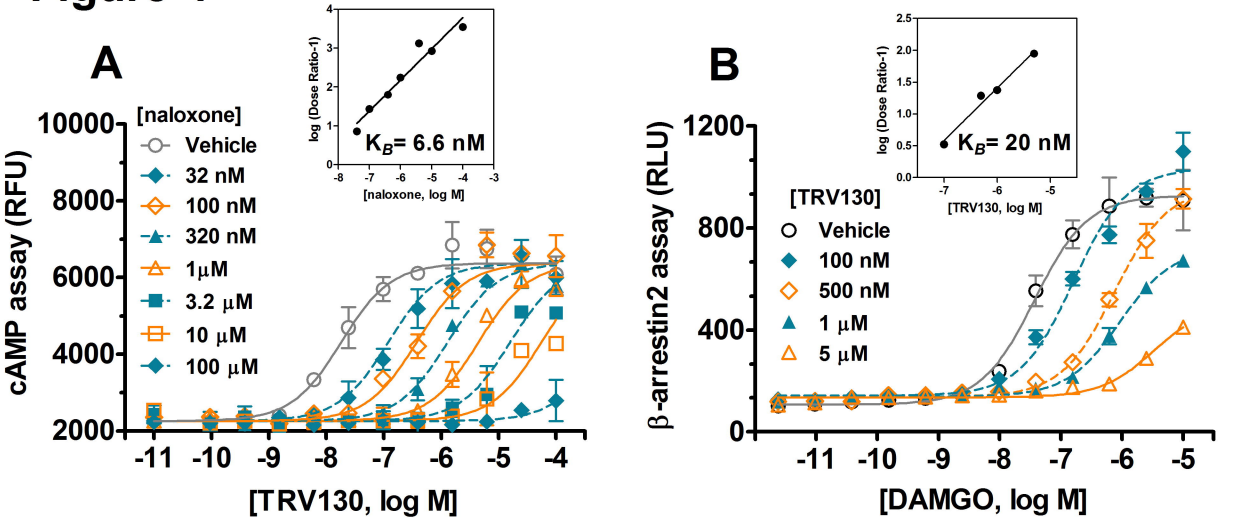
A
[naloxone]
Vehicle
32 nM
100 nM
320 nM
1μM
3.2 μM
10 μM
100 μM
cAMP assay (RFU)
[TRV130, log M]
log (Dose Ratio-1)
[naloxone, log M]
K_B= 6.6 nM
B
[TRV130]
Vehicle
100 nM
500 nM
1 μM
5 μM
β-arrestin2 assay (RLU)
[DAMGO, log M]
log (Dose Ratio-1)
[TRV130, log M]
K_B= 20 nM

Figure 5

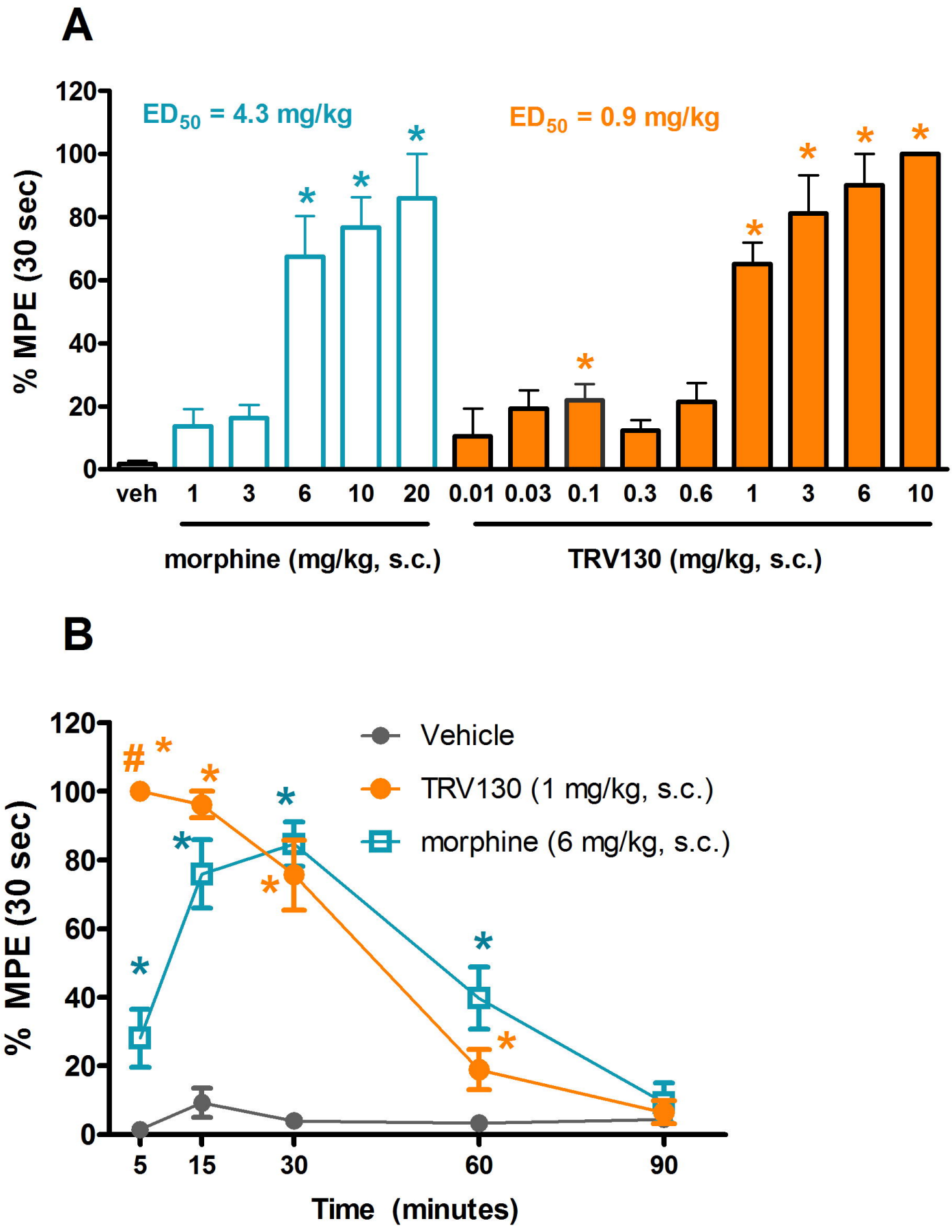
A
ED50 = 4.3 mg/kg
ED50 = 0.9 mg/kg
% MPE (30 sec)
120
100
80
60
40
20
0
veh
1
3
6
10
20
0.01
0.03
0.1
0.3
0.6
1
3
6
10
morphine (mg/kg, s.c.)
TRV130 (mg/kg, s.c.)
B
Vehicle
TRV130 (1 mg/kg, s.c.)
morphine (6 mg/kg, s.c.)
% MPE (30 sec)
5
15
30
60
90
Time (minutes)

Figure 6

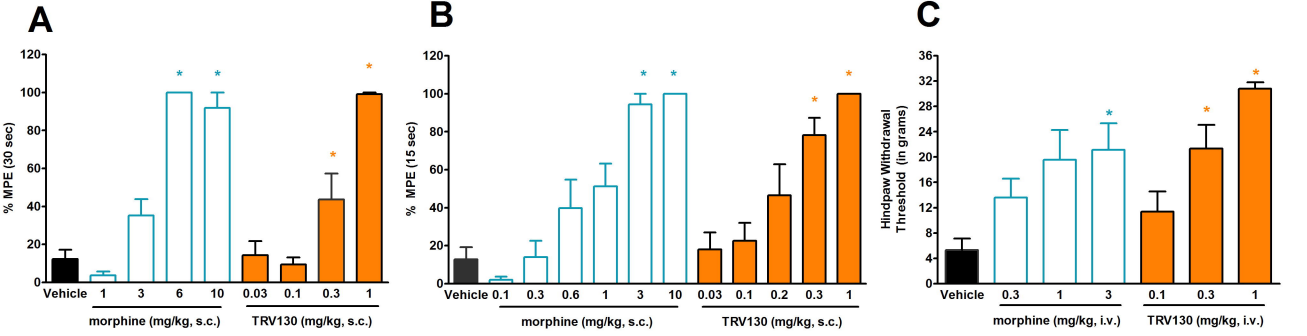
A
% MPE (30 sec)
120
100
80
60
40
20
0
Vehicle
1
3
6
10
0.03
0.1
0.3
1
morphine (mg/kg, s.c.)
TRV130 (mg/kg, s.c.)
B
% MPE (15 sec)
120
100
80
60
40
20
0
Vehicle
0.1
0.3
0.6
1
3
10
0.03
0.1
0.2
0.3
1
morphine (mg/kg, s.c.)
TRV130 (mg/kg, s.c.)
C
Hindpaw Withdrawal Threshold (in grams)
36
32
28
24
20
16
12
8
4
0
Vehicle
0.3
1
3
0.1
0.3
1
morphine (mg/kg, i.v.)
TRV130 (mg/kg, i.v.)

Figure 7

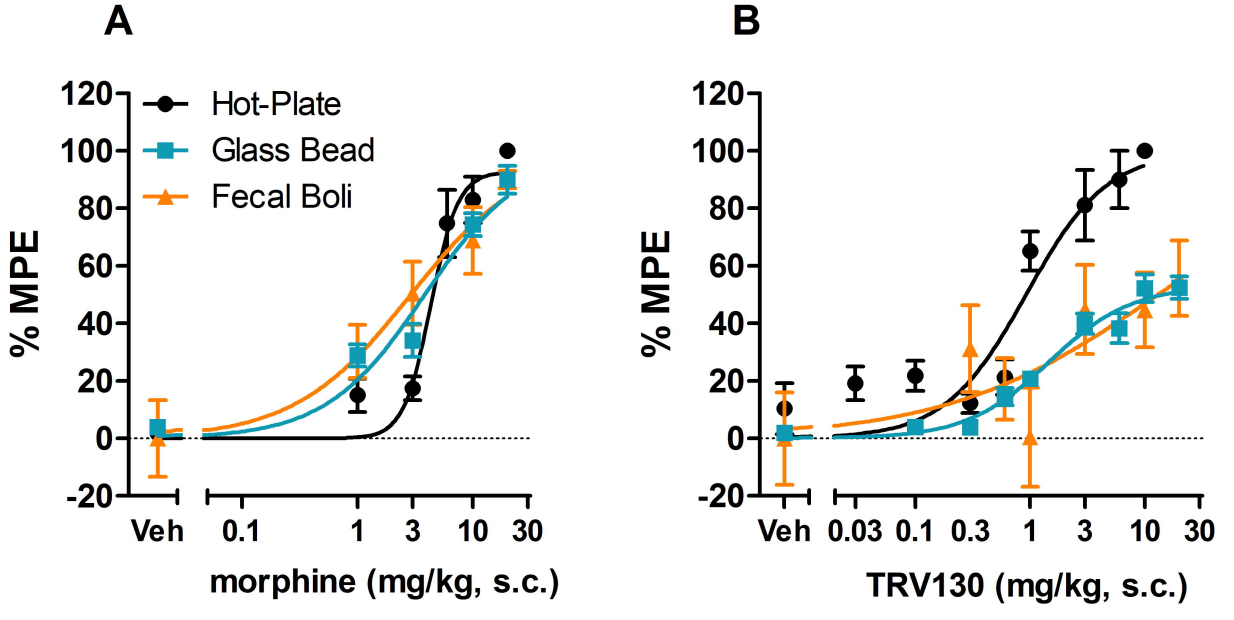
A
B
Hot-Plate
Glass Bead
Fecal Boli
% MPE
120
100
80
60
40
20
0
-20
Veh
0.1
1
3
10
30
morphine (mg/kg, s.c.)
0.03
0.3
TRV130 (mg/kg, s.c.)

Figure 8

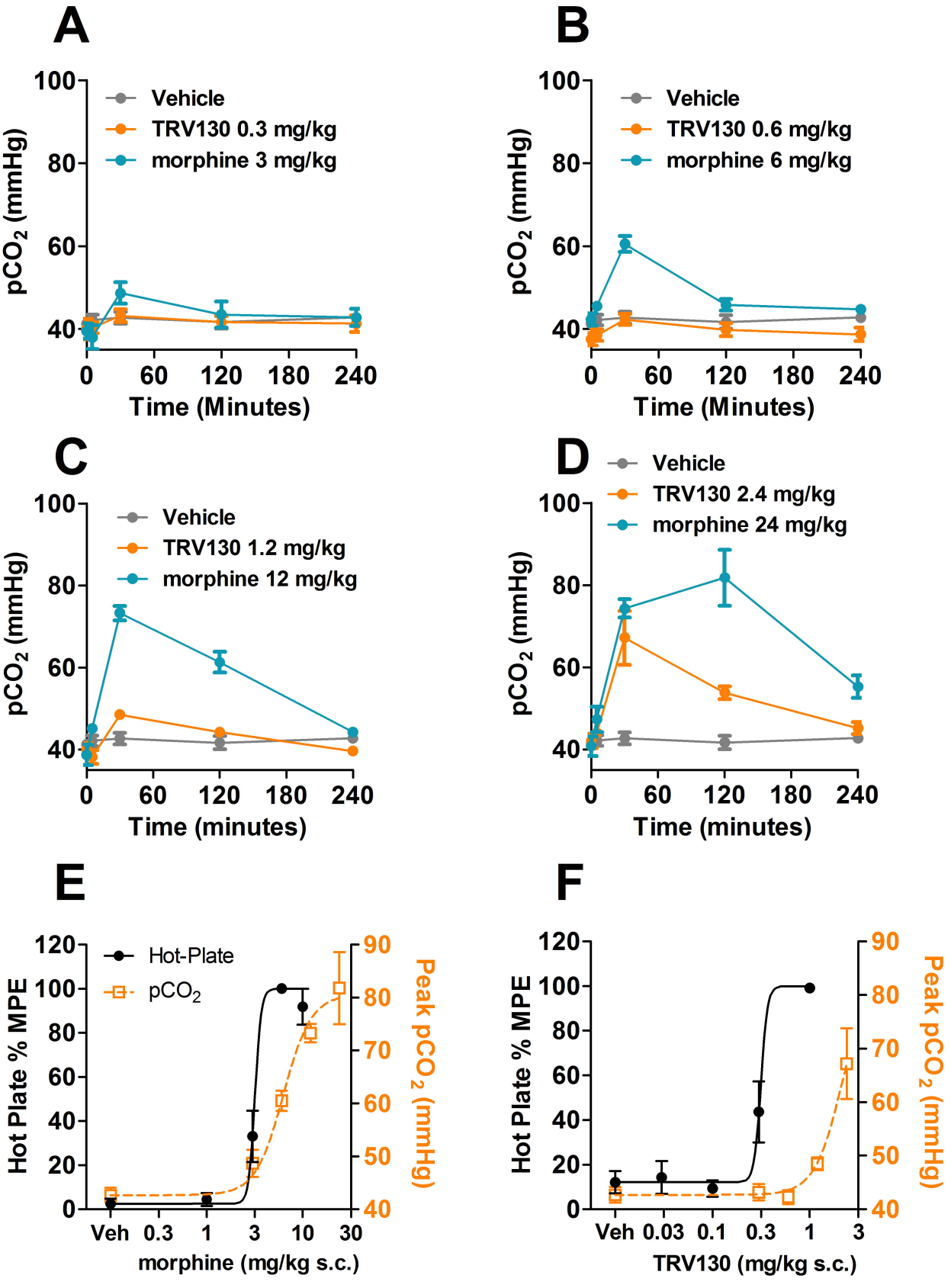
A
Vehicle
TRV130 0.3 mg/kg
morphine 3 mg/kg
pCO2 (mmHg)
Time (Minutes)
B
Vehicle
TRV130 0.6 mg/kg
morphine 6 mg/kg
pCO2 (mmHg)
Time (Minutes)
C
Vehicle
TRV130 1.2 mg/kg
morphine 12 mg/kg
pCO2 (mmHg)
Time (minutes)
D
Vehicle
TRV130 2.4 mg/kg
morphine 24 mg/kg
pCO2 (mmHg)
Time (minutes)
E
Hot-Plate
pCO2
Hot Plate % MPE
Peak pCO2 (mmHg)
Veh 0.3 1 3 10 30
morphine (mg/kg s.c.)
F
Hot Plate % MPE
Peak pCO2 (mmHg)
Veh 0.03 0.1 0.3 1 3
TRV130 (mg/kg s.c.)